ELSEVIER

Biochimica et Biophysica Acta 1570 (2002) 19–26

BIOCHIMICA ET BIOPHYSICA ACTA
BBA

www.bba-direct.com

Iodination significantly influences the binding of human transferrin to the transferrin receptor

Hendrik Fuchs [1], Reinhard Geßner *

Institut für Laboratoriumsmedizin und Pathobiochemie, Medizinische Fakultät Charité der Humboldt-Universität zu Berlin, Campus Virchow-Klinikum, Augustenburger Platz 1, D-13353 Berlin, Germany

Received 22 February 2001; received in revised form 25 September 2001; accepted 13 December 2001

Abstract

The human transferrin receptor (TfR) and its ligand, the serum iron carrier transferrin, serve as a model system for endocytic receptors. Although the complete structure of the receptor's ectodomain and a partial structure of the ligand have been published, conflicting results still exist about the magnitude of equilibrium binding constants, possibly due to different labeling techniques. In the present study, we determined the equilibrium binding constant of purified human TfR and transferrin. The results were compared to those obtained with either iodinated TfR or transferrin. Using an enzyme-linked assay for receptor–ligand interactions based on the published direct calibration ELISA technique, we determined an equilibrium constant of $K_d = 0.22$ nM for the binding of unmodified human Tf to surface-immobilized human TfR. In a reciprocal experiment using soluble receptor and surface-bound transferrin, a similar constant of $K_d = 0.23$ nM was measured. In contrast, covalent labeling of either TfR or transferrin with ^{125}I reduced the affinity 3–5-fold to $K_d = 0.66$ nM and $K_d = 1.01$ nM, respectively. The decrease in affinity upon iodination of transferrin is contrasted by an only 1.9-fold decrease in the association rate constant, suggesting that the iodination affects rather the dissociation than the association kinetics. These results indicate that precautions should be taken when interpreting equilibrium and rate constants determined with covalently labeled components.

Keywords: Dissociation constant; Kinetics; Receptor–ligand interaction; Iodination; Enzyme-linked immunosorbant assay; Enzyme-linked assay for receptor–ligand interactions

1. Introduction

The transferrin receptor (TfR) mediates the cellular uptake of iron by binding and internalization of the serum iron transport protein transferrin (Tf). Within the acidic microenvironment of early endosomes, iron ions dissociate from transferrin and are transported to the cytoplasm. The remaining TfR–apo-transferrin complex recycles back to the cell surface where apo-transferrin dissociates and the receptor becomes capable of binding again ferritransferrin [1,2]. The human TfR is a class II transmembrane glycoprotein composed of two identical subunits that are covalently linked by two disulfide bonds [3]. Each subunit of the extracellular region binds one transferrin molecule. Structurally, the extracellular region is composed of three distinct domains, organized so that the TfR dimer has a butterfly-like shape [4]. The butterfly-like domain is kept at a distance of 2.9 nm from the plasma membrane by a molecular stalk [5] and carries three *N*-glycans [6,7]. The stalk contains a single *O*-glycan at threonine-104 [8,9].

The binding of human transferrin to its receptor has already been quantified in numerous studies, all of them employing receptor molecules on primary cells, cell lines or cell extracts. Depending on the method extremely different equilibrium dissociation constants have been determined: K_d of 20–29 nM for the binding of transferrin to human placental syncytiotrophoblasts [10], K_d of 1.1 nM for a microsomal preparation from human breast cancer cells [11], K_d of 0.42 nM for a Triton lysate from human

Abbreviations: TfR, transferrin receptor; Tf, transferrin; EARLI, enzyme-linked assay for receptor–ligand interactions; PBS, phosphate-buffered saline (150 mM NaCl, 10 mM phosphate, pH 7.5); PBST, PBS+0.05% Tween 20; 8-POE, octylpolyoxyethylene; PAGE, polyacrylamide gel electrophoresis

* Corresponding author. Fax: +49-30-450-569907.

E-mail address: gessner@charite.de (R. Geßner).

[1] Present address: Institut für Klinische Chemie und Pathobiochemie, Universitätsklinikum Benjamin Franklin, Freie Universität Berlin, D-12200 Berlin, Germany.

0304-4165/02/$ – see front matter
PII: S0304-4165(02)00146-0

placenta [12] and K_d of 0.12 nM for a Triton lysate of HL60 cells [13]. In contrast to the equilibrium dissociation constants, experimentally determined rate constants were rather uniform. The internalization of transferrin occurs with $k_c = 0.20–0.23$ min^{-1} [14–16]. Since the binding of transferrin takes place with the same rate (0.23 min^{-1}) [14], it can be assumed that the complex formation is the rate-determining step.

The large variation of equilibrium binding constants determined in previous studies with whole cells and cell extracts may reflect the influence of other mechanisms on the apparent binding constant, such as competition by endogenous transferrin [12], the binding of transferrin to other receptors like the asialoglycoprotein receptor [17,18] and the partial intracellular degradation of endocytosed transferrin. Since, on the other hand, some of these modifying mechanisms, such as endocytosis, have often been quantified by studying transferrin uptake, it appears to be very important to have exact numbers for the Tf-TfR binding reaction in order to deconvolute related cellular processes.

Very accurate measurements can be obtained by using highly purified components. The equilibrium binding constant can then be easily determined with common methods such as Scatchard analysis. However, this method requires the quantitation of the bound fraction of the soluble component which is conveniently achieved by radioactive labeling. Covalent labeling, on the other hand, bears the risk of modifying the binding properties [19–22]. To avoid this problem, we had recently developed an alternative method (direct calibration (dc) ELISA) to quantify the bound fraction of the ligand without the need of any modification [23].

Based on this method we now developed a new enzyme-linked assay for receptor–ligand interactions (EARLI, see Sections 2 and 3). In the current study, we applied the EARLI to determine the equilibrium constant for the binding of transferrin to its receptor. The result was validated using either transferrin or the receptor as the soluble component. Comparing these results to those obtained by a Scatchard analysis of ^{125}I-labeled transferrin or transferrin receptor revealed that the covalent modification reduced the binding affinity 3–5-fold.

2. Materials and methods

2.1. Materials

Transferrin was purchased from Sigma (St. Louis, MO, USA), polyclonal immunoglobulins from Dako (Glostrup, Denmark), monoclonal rabbit anti-mouse κ-chain antibodies (clone H139.52.1) from Dianova (Hamburg, Germany) and monoclonal mouse anti-transferrin antibodies MAB033-19/1 from Chemicon International (Temecula, CA, USA). Monoclonal antibodies OKT9 were prepared as described previously [24]. Fetal calf serum was a product of Gibco BRL (Paisley, UK). Iodo-Gen was obtained from Pierce (Rockford, IL, USA) and CNBr-activated Sepharose 4B from Pharmacia (Uppsala, Sweden). 3,3′,5,5′-Tetramethylbenzidine was from Merck (Darmstadt, Germany) and octylpolyoxyethylene (8-POE) (Rosenbusch-Tenside) from Bachem (Heidelberg, Germany).

2.2. Preparation of a ferri-transferrin affinity column

Iron saturation of transferrin was performed basically according to the method of Karin and Mintz [25]. However, the buffer (phosphate-buffered saline (PBS)) was supplemented with 1 mM $NaHCO_3$, since we had found that in this case saturation occurs more than 10 times faster and was more quantitative (unpublished data). Coupling of ferri-transferrin to CNBr-activated Sepharose was performed according to the manufacturer's instructions.

2.3. Purification of the transferrin receptor

Human transferrin receptor was solubilized and separated from bound transferrin as described by Turkewitz et al. [26]. The solubilized receptor was loaded onto a ferri-transferrin Sepharose affinity column (prepared as described above). For elution of functional human TfR with high binding activity, the receptor was eluted under non-denaturing conditions with 2 M KCl, 1% 8-POE in PBS, pH 7.5. Remaining receptor was subsequently eluted with 0.5 M KSCN, 1% 8-POE in PBS, pH 7.5. However, the latter fraction was shown to be non-functional (see Section 3) and was not used for any binding experiments. High salt was removed on PD-10 columns (Pharmacia) equilibrated with PBS, 1% 8-POE and stored at 4°C.

2.4. Labeling of transferrin and TfR with ^{125}I

Human transferrin (200 μg) was iodinated with 2.2 MBq Na^{125}I using the Iodo-Gen method described by Fraker and Speck [27]. The quality of the labeled protein was determined by sodium dodecyl sulfate (SDS)–polyacrylamide gel electrophoresis (PAGE) and autoradiography (Fig. 1A, lanes 11 and 12). More than 90% of the initially applied activity could be recovered from the corresponding excised gel fragment. Human TfR (88 μg) was iodinated with 1.5 MBq Na^{125}I accordingly.

2.5. Labeling of transferrin with ^{59}Fe

50 μl (185 kBq) of a $^{59}FeCl_3$ solution in 1 M HCl were added to 16.5 μl of 5.2 mM sodium citrate and the pH was then raised to 7.8 by adding 13.5 μl 0.4 M sodium carbonate. This solution was mixed with 20 μl apo-transferrin (25 mg/ml) and incubated at room temperature for 45 min. Unbound iron was removed by tandem gel filtration on Sephadex G-25.

2.6. EARLI

TfR samples used in this assay were exclusively from fractions of the elution with KCl. In general, all solid phase assays were performed in modular 96-well microtiter plates (Nunc) at room temperature. Sample volumes were 100 μl per well if not noted otherwise. Wash procedures between any two successive incubation steps included three wash steps with 250 μl PBS+0.05% Tween 20 (PBST), followed by a 5 min incubation with 150 μl PBST and three more 250 μl PBST wash steps. The microtiter plates were constantly agitated during all incubation steps in a Varishaker Incubator at medium speed (Dynatech, Guernsey, UK).

To check a possible influence of immobilization on the binding properties either the receptor or transferrin were immobilized. Either 100 ng/well TfR or 500 ng/well ferri-transferrin were incubated in Nunc-immuno modules MaxiSorp U16 for enzyme-linked assays and in Nunc-immuno BreakAparts MaxiSorp C8 for assays with radioactive compounds. Coating was performed in PBS for 1.5 h. Excess binding sites were blocked for 30 min with 200 μl PBS containing 3% bovine serum albumin and 10% fetal calf serum.

Subsequently, transferrin (or in the reverse assay the receptor) was incubated in PBST for 2.5 h; concentrations are given in the figures. Samples were incubated for 30 min with 16 ng/well monoclonal antibodies MAB033 against human transferrin in PBST and then 30 min with 5 ng/well peroxidase-conjugated monoclonal rabbit anti-mouse κ-chain antibodies again in PBST. In the reverse assay, the monoclonal antibody OKT9 was used instead of MAB033. For the following enzyme-catalyzed reaction, a 0.02% solution of 3,3′,5,5′-tetramethylbenzidine in a 40 mM potassium citrate buffer, pH 3.95, containing 0.01% H_2O_2 was used [28]. The reaction was usually stopped after 10 min by adding 50 μl 2 M sulfuric acid to each well. Absorbance was measured at 450 nm in a multi-channel photometer (MR 7000, Dynatech, Denkendorf, Germany) and corrected for light scattering effects by subtracting the absorbance at 490 nm. Absorbance readings in excess of 1.5 were avoided by adjusting the incubation period of the enzyme reaction, if required.

When using radioactive compounds (^{125}I- and ^{59}Fe-labeled), modules were broken apart into single wells and the activity of each well was measured separately in a γ-counter (Berthold LB 2111, Bad Wildbad, Germany).

All error bars refer to the standard deviation of several independent measurements as indicated in the figure legends. The error bars do not include any errors that do not affect the statistical error such as unavoidable inaccuracies of the time of data recording (affecting in particular the kinetics) and experimental errors of ligand dilutions (affecting in particular the Scatchard analysis). Thus, regression curves may escape error bars, because the true error is considerably larger than the statistical error displayed in the figures. The errors of the calculated rate and equilibrium constants were derived from the regression coefficient using a standard software for statistical calculations (StatView 4.5, SAS Institute Inc., Carg, NC, USA). A thorough error analysis of several methods including Scatchard and EARLI revealed that small systematic errors can lead to a deviation of the equilibrium constant of up to 30%, which is considerably larger than the standard deviation from repeated measurements. In comparison, the EARLI analysis appears to be more robust against systematic errors [29].

2.7. Direct calibration of the EARLI and determination of the dissociation constants (dcEARLI)

To calibrate the relative absorbance signal (i.e. to determine the constant calibration factor c that defines the relationship between absorbance (A) and absolute amount of bound ligand (RL): $RL_n = c \cdot A_n$), a defined amount of ligand (2.8 ng ferri-transferrin or 4 ng TfR) was allowed to bind for various incubation periods to the immobilized partner (TfR and ferri-transferrin, respectively). Subsequently, the supernatant was transferred to another, identically coated well and again incubated for the same time. Seven transfers were performed for short incubation periods and a minimum of three for longer ones. The bound ligand was detected as described above. Internal calibration and calculation of dissociation and rate constants were performed as described recently [23]. Briefly, in the transfer assay the sum of all absorbance readings is related to the initial amount of ligand (L_0) by the calibration factor c: $L_0 = \sum_{n=1}^{\infty} \mathrm{RL}_n = c \cdot \sum_{n=1}^{\infty} A_n$. Thus, c can be calculated by $c = L_0/A_1 \cdot (1-F)$. F is the transfer factor determined from the slope (corresponding to ln F) in the transfer plots (Figs. 3A and 4A). In order to avoid extended incubation periods, the transfer assay was performed with several short incubation periods and the data were extrapolated in the F-plot (Figs. 3B and 4B) to an infinite binding period corresponding to equilibrium conditions (for details, see [23]).

2.8. SDS–PAGE, Western blot and protein determination

Samples were prepared according to Laemmli [30] and separated by 7.5% SDS–PAGE. Staining was performed with Coomassie blue R-250 after fixing with 20% trichloroacetic acid. For Western blotting, the proteins were transferred to a cellulose nitrate membrane (BA 85, 0.45 μm, Schleicher and Schuell, Dassel, Germany) that was blocked thereafter with PBST containing 3% bovine serum albumin and 10% fetal calf serum. Transferrin was detected with polyclonal rabbit anti-transferrin antibodies (60 μg/ml) and human TfR with OKT9 (6 μg/ml). Secondary, peroxidase-conjugated antibodies were stained for approx. 10 min with 50 mM Tris–HCl, pH 7.5, 200 mM

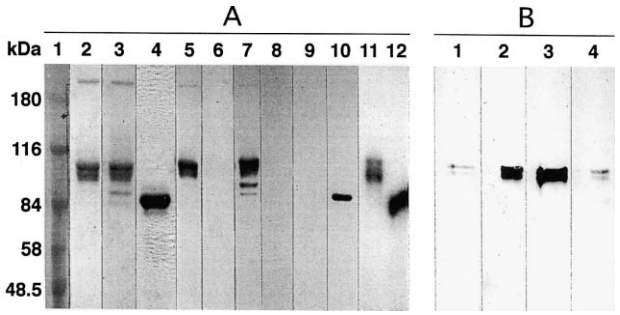

Fig. 1. Control of purification, labeling and binding capacity of human TfR and Tf. (A) SDS–PAGE of KCl- and KSCN-eluted TfR, and of Tf. Lanes: 1–4, Coomassie stain of molecular mass markers (1), KCl-eluted TfR (2), KSCN-eluted TfR (3) and Tf (4); 5–10, Western blot of KCl-eluted TfR (5, 6), KSCN-eluted TfR (7, 8) and of Tf (9, 10) using anti-TfR monoclonal antibodies OKT9 (5, 7, 9) or anti-Tf rabbit antisera (6, 8, 10); 11 and 12, autoradiogram of ^{125}I-labeled KCl-eluted TfR (11) and Tf (12). (B) Rebinding of KCl- (lanes 1 and 2) and KSCN-eluted (lanes 3 and 4) TfR to a ferri-Tf gel matrix. Non-bound (lanes 1 and 3) and rebound fractions (lanes 2 and 4) were detected in a Western blot after separation of the proteins by SDS–PAGE. Wash fractions did not contain any detectable amounts of protein and are not displayed.

KCl, 0.06% 4-chloro-1-naphthol (stock solution 0.3% in methanol), 0.01% H_2O_2.

Protein concentrations were determined as duplicates on microtiter plates using the Pierce BCA protein assay (No. 23225, Pierce) and the appropriate microscale protocol of the manufacturer.

3. Results

3.1. Purification of human transferrin receptor

TfR was eluted from the ligand affinity column under non-denaturing conditions (2 M KCl). Subsequently, the column was washed with a strongly chaotropic salt solution (0.5 M KSCN) to remove any remaining receptor. Fig. 1A (lanes 2 and 3) shows that both fractions exhibit a very similar gel electrophoretic separation pattern: the majority of the protein is concentrated in two intense bands with a molecular mass of about 93 kDa, indicating some microheterogeneity possibly due to variations in the posttranslational modifications [6,8,9,31,32]. In addition, a faint band is seen at about 185 kDa, obviously representing a covalently linked receptor dimer that persists under reducing conditions (2% mercaptoethanol). Only the KSCN-eluted TfR fraction shows an additional band at about 85 kDa that was identified by N-terminal protein sequencing (data not shown) as the human serum transferrin receptor [33]. A comparison of the Coomassie protein staining pattern (Fig. 1A, lanes 2–4) with the results of Western blots using anti-TfR and anti-Tf antibodies (Fig. 1A, lanes 5–10) reveals the high purity of both TfR preparations without any detectable contaminants, including human transferrin (Fig. 1A, lanes 6 and 8).

A semi-quantitative assessment of the rebinding capacity of purified TfR to Sepharose-coupled transferrin (Fig. 1B) showed that more than 95% of the KCl-eluted receptor remained active, while less than 5% of the KSCN-eluted receptor was able to bind again to the immobilized ferri-transferrin. Due to this result, only KCl-eluted TfR was used for further studies. The protein was stored at 4°C, since it was stable under this condition for many weeks without any precipitation or detectable loss of binding activity, whereas a single freeze and thaw cycle reduced its binding activity by more than 90% (data not shown).

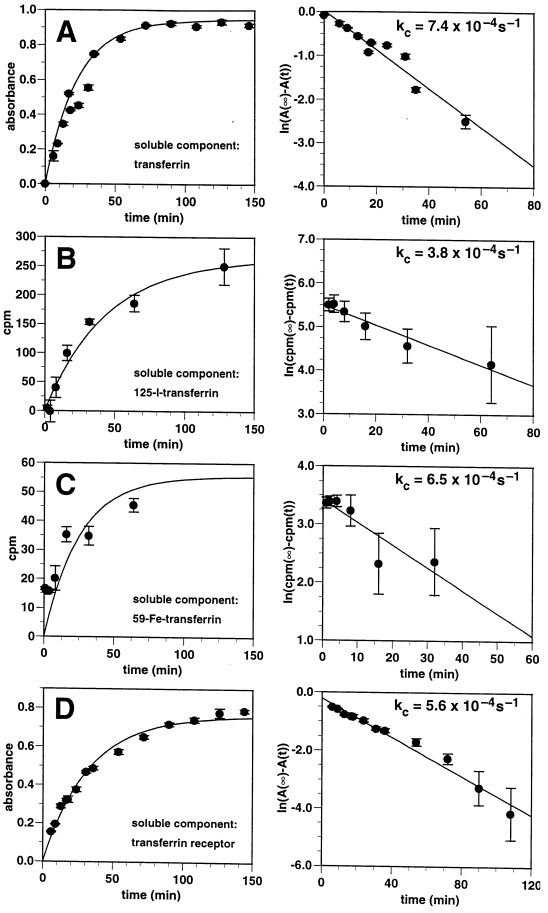

Fig. 2. Determination of the transferrin–TfR complex formation rate constant. Unlabeled (A), ^{125}I-labeled (B) and ^{59}Fe-labeled transferrin (C) were incubated at increasing incubation periods to immobilized transferrin receptor. The rate constant was calculated from a semi-logarithmic plot of unbound transferrin versus time (panels on the right). The slope indicates a rate constant of $k_c = 7.4(\pm 0.5)\times 10^{-4}$ s^{-1} for the binding of unlabeled transferrin to its receptor, of $k_c = 3.8(\pm 0.2)\times 10^{-4}$ s^{-1} for the binding of ^{125}I-Tf and of $k_c = 6.5(\pm 1.8)\times 10^{-4}$ s^{-1} for the binding of ^{59}Fe-Tf. Corresponding to the radioreceptor assay, rate constants were also determined in the reciprocal EARLI (D, with Tf coated) and found to be $k_c = 5.6(\pm 0.2)\times 10^{-4}$ s^{-1}. Error bars indicate the standard deviation of duplicates (B), triplicates (A,D) or quadruplicates (C). The error of k_c was derived from the regression coefficient using a standard software for statistical calculations (StatView v4.5).

3.2. Design and verification of the EARLI

The assay is based on the dcELISA we have developed recently [23]. However, instead of analyzing the binding of an antibody to its respective immobilized antigen, the EARLI was designed to quantify by a simple and reliable method the binding of a ligand, i.e. transferrin, to its receptor, i.e. TfR. Bound ligand was determined using a high affinity primary and an enzyme-linked secondary antibody. The calibration of the colorimetric readouts was achieved in analogy to the dcELISA by repeated transfer of unbound ligand to another well and kinetically based compensation for the non-equilibrium conditions of the subsequent binding reactions [23]. Each of the following parameters was optimized independently: amount of protein and length of incubation period necessary to saturate the solid phase, composition of the blocking buffer, concentration and incubation period of the primary and secondary enzyme-linked antibodies, stability of the complex between receptor, ligand and antibodies, kinetics of the dissociation of $^{59}Fe^{3+}$ from ferri-transferrin, and, finally, linearity between the amount of bound ligand and the recorded signal. A further validation was achieved by performing the reciprocal EARLI with immobilized transferrin and solubilized receptor.

Some results verifying the reliability of the EARLI should be mentioned briefly. Using the best blocking buffer, background absorbance readings were constantly smaller than 0.03 and varied within one series by less than 0.01. Consequently, even very small signals could be corrected for background absorption with high accuracy. The possible dissociation of human TfR from immobilized transferrin during wash and incubation steps was monitored over a time period of 80 min by replacing the TfR solution by PBST and was found to be less than 3%. In analogy, the stability of the whole complex formed by TfR, transferrin, primary and secondary antibodies was experimentally determined by delaying the final enzyme reaction by an additional PBST incubation step of 60 min. This delay reduced the relative signal to 68(±6)%, which by itself does not influence the final result, since enzyme-linked assays are anyhow based on relative signals. Thus, the final result is only affected by the variation of the factor within one series of data. However, the observed variations affected the final result by less than 2%.

To determine the dissociation of Fe^{3+} from ferri-transferrin while performing the EARLI, increasing amounts of ^{59}Fe-labeled ferri-transferrin were immobilized in parallel on two identical plates. While one plate was washed only once and then set aside, the other was run through the regular EARLI procedure including binding and detecting the TfR by the enzyme-linked assay. Just before adding the substrate solution, the procedure was interrupted and both plates were counted. The average ratio of the activity of corresponding wells was close to one (<1.05), indicating no detectable loss of $^{59}Fe^{3+}$.

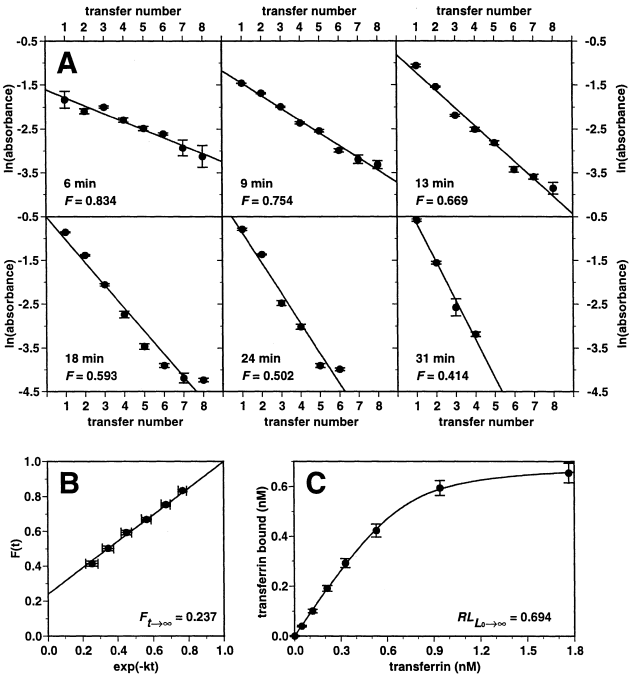

Fig. 3. Determination of the Tf–TfR complex equilibrium dissociation constant by the EARLI. (A) Transfer plot: 2.8 ng ferri-transferrin (L_0) was incubated on TfR-coated wells (100 ng) and after each incubation period the supernatant was transferred to the next TfR-coated well. This procedure was repeated several times for six different incubation periods (6–31 min). Each data point represents the mean value of three samples ±S.D. The calibration factor c was calculated independently for all six time variations and averaged to $\bar{c}=0.339$ (±0.016) nM (for details, see [23]). (B) F plot: the applied rate constant k_c was already determined in Fig. 2A. The time-independent transfer factor F was derived from the intersection of the regression curve with the y-axis and determined to $F=0.237$ (±0.047). The error was calculated from the regression coefficient. (C) Saturation curve: immobilized TfR was incubated with various amounts of unlabeled ferri-transferrin for 2.5 h. Each data point represents the average of six measurements ±S.D. Using the saturation concentration ($\bar{c}\times A_{L_0\to\infty}$) of 0.694 (±0.027) nM, the calibration factor $\bar{c}$, and the time-independent transfer factor F, the equilibrium dissociation constant was calculated to $K_d=0.215$ (±0.053) nM.

3.3. Determination of complex formation rate constants

Kinetic constants are important for characterizing the binding of transferrin to its cognate receptor and essential for determining equilibrium constants by direct calibration [23]. Upon variation of the incubation period, the complex formation rate constant for the binding of transferrin to surface-immobilized TfR was determined to be $k_c = 7.4(\pm 0.5)\times 10^{-4}$ s^{-1} (Fig. 2A). A similar experiment with ^{125}I-labeled transferrin and radiometric quantitation led to $k_c = 3.8(\pm 0.2)\times 10^{-4}$ s^{-1} (Fig. 2B). In order to analyze whether the slower binding of ^{125}I-Tf is due to the covalent modification or to the different quantitation methods, we used chemically non-modified ^{59}Fe-Tf as a reference system. Applying the same radiometric quantitation that was used for ^{125}I-transferrin, a rate constant of $k_c = 6.5(\pm 1.8)\times 10^{-4}$ s^{-1} was determined for the binding

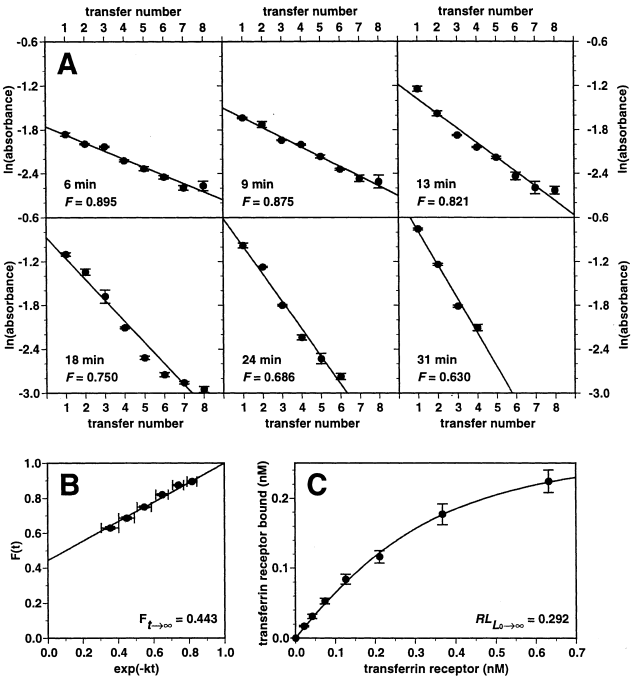

Fig. 4. Determination of the Tf–TfR complex equilibrium dissociation constant by the reciprocal EARLI (with coated transferrin). (A) Transfer plot: 4 ng TfR (L_0) was incubated on transferrin-coated wells (500 ng) and then transferred to the next transferrin-coated well as described in Section 2. Three independent measurements were averaged for each data point, error bars indicate S.D. The calibration factor was calculated to $\bar{c} = 0.151 \pm 0.009$ nM. (B) F plot: F_i was plotted versus $e^{-k_c t}$ with k_c from Fig. 2D. The transfer factor was determined to $F = 0.443$ (± 0.063). (C) Saturation curve: immobilized ferri-transferrin was incubated with various amounts of unlabeled TfR for 2.5 h. Each data point represents the average of six measurements $\pm$S.D. Using the saturation concentration ($\bar{c} \times A_{L_0\to\infty}$) of 0.292 ($\pm 0.012$) nM, the calibration factor, and the transfer factor, the dissociation constant was calculated to $K_d = 0.233$ (± 0.069) nM.

of ^{59}Fe-Tf to the transferrin receptor (Fig. 2C). This binding rate is within the experimental error identical to that of unlabeled transferrin.

In a reciprocal EARLI, the binding of soluble TfR to immobilized transferrin was analyzed. The slightly lower association rate constant of $k_c = 5.6(\pm 0.2) \times 10^{-4}$ s^{-1} (Fig. 2D) versus $k_c = 7.4 \times 10^{-4}$ s^{-1} for soluble transferrin may reflect a slower diffusion of the large solubilized receptor dimer (225 kDa including bound detergent molecules [24] as compared to 80 kDa of transferrin).

3.4. Determination of the equilibrium dissociation constants

Similar to the determination of rate constants, we also measured equilibrium constants with either unlabeled molecules in the EARLI or radiolabeled compounds in a radioreceptor assay. The dcEARLI was first used to analyze the binding of Tf to immobilized TfR (Fig. 3). In total, six transfer assays were performed with ligand incubation periods (t_i) varying between 6 min and 31 min (Fig. 3A). The derived transfer factors F_{t_i} were plotted over $e^{-k_c \cdot t}$ in order to determine the transfer factor F for equilibrium conditions ($F = F_{t\to\infty}$) (Fig. 3B). Combining this result with that of the ligand saturation curve (Fig. 3C) revealed an equilibrium dissociation constant of

$$K_d = \frac{F \cdot A_{L_0\to\infty} \cdot \bar{c}}{1-F} = 215(\pm 53)\ \text{pM}$$

with

$$\bar{c} = \frac{\sum_1^i \frac{L_0 \cdot (1-F_{t_i})}{A_{1_i}}}{i}$$

where F is the transfer factor, $A_{L_0\to\infty}$ the absorbance at ligand saturation, L_0 the initial ligand concentration, A_1 the first absorbance in the transfer assay and i the number of transfer experiments. In order to validate this result, a reciprocal dcEARLI with soluble TfR was performed. This experiment yielded a similar equilibrium constant of $K_d = 233$ (± 69) pM (Fig. 4). The similarity of the equilibrium constants obtained with the normal and reciprocal EARLI suggests that the binding between transferrin and TfR does not depend on which binding partner is immobilized.

In order to investigate whether iodination influences the equilibrium dissociation constant, a Scatchard analysis [34] was performed with ^{125}I-Tf (Fig. 5). The Scatchard plot (Fig. 5B) revealed an equilibrium binding constant of $K_d = 1006$ (± 33) pM, indicating a decrease in affinity by a factor of 4.7. Unfortunately, the effect of transferrin iodination on the binding could not be verified in analogy to the kinetic studies with ^{59}Fe-labeled transferrin, since the specific activity of the commercially available $^{59}Fe^{3+}$ was too low for an accurate determination of equilibrium constants. The reciprocal experiment employing soluble, ^{125}I-labeled TfR and surface-immobilized Tf, yielded a $K_d = 659$ (± 22) pM (Fig. 6). This 2.8-fold reduction in affinity underlines the effect of the covalent modification. Although the result suggests a common mechanism, one should bear in mind that in this case the receptor and not the ligand transferrin was chemically modified.

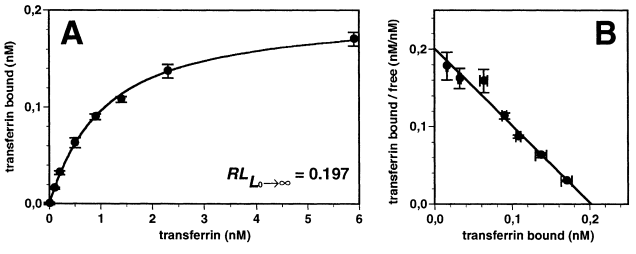

Fig. 5. Determination of the ^{125}Tf–TfR complex dissociation constant by a radioreceptor assay with immobilized TfR. (A) Immobilized TfR was incubated with various amounts of iodinated ferri-transferrin for 2.5 h. Each data point represents the average of six measurements $\pm$S.D. The specific radioactivity was used to determine absolute amounts of bound ligand. (B) The dissociation constant of the complex was derived by Scatchard analysis and calculated to $K_d = 1.01$ (± 0.03) nM. The error of K_d was derived from the regression coefficient.

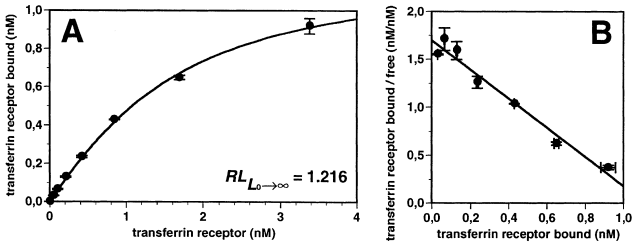

Fig. 6. Determination of the Tf–^{125}TfR complex dissociation constant by a radioreceptor assay with immobilized transferrin. (A) Immobilized transferrin was incubated with various amounts of iodinated TfR for 2.5 h. Each data point represents the average of two measurements ± S.D. The specific radioactivity was used to determine absolute amounts of bound ligand. (B) Scatchard plot. The dissociation constant of the complex was determined to $K_d = 0.66$ (± 0.02) nM.

In general, a systematic deviation from linearity in the Scatchard plot indicates a more complicated binding model with two or more ligand populations of different affinity to the receptor. Although our data reveal clear linearity and the small deviations are randomly and not systematically distributed, we additionally used the program LIGAND for non-linear analysis of binding constants. For the binding of ^{125}I-TfR to immobilized transferrin, the data calculated by LIGAND were virtually the same as in the linear Scatchard plot. Even when assuming three different ligand populations, the calculated dissociation constants for the three 'different' ligands were 658 pM, 662 pM and 667 pM, indicating that only a single ligand population with a K_d of 0.66 nM is present. For the binding of iodinated transferrin to immobilized TfR, a K_d of 0.93 nM was calculated for the one-ligand model. However, the best fit was calculated for the two-ligand model. Two solutions have exactly the same lowest mean square ($K_d(1) = 0.97$ nM, $K_d(2) = 1.38$ nM and $K_d(1) = 0.83$ nM, $K_d(2) = 1.09$ nM), indicating that an unequivocal result cannot be obtained. Although it remains unsettled if the results of the two-ligand model are a consequence of random data scattering or of a true population effect, the quintessence that iodination of transferrin or of TfR leads to a significantly higher dissociation constant is undoubtedly confirmed by this alternative numeric analysis.

4. Discussion

In the present study, we have determined the kinetic and equilibrium constants for the binding of human transferrin to the human TfR. In addition, we have quantified the effect of covalent modifications with ^{125}I on the apparent binding constants. Whereas previous studies of other groups utilized whole cells or cell extracts, we established a new enzyme-based assay for quantifying receptor–ligand interactions (EARLI) without the need of covalent modifications. We used highly purified components and validated the assay by analyzing every individual experimental step separately with regard to its influence on the final result. The standard error of the rate constants was, with one exception, found to be less than 7% and that of equilibrium dissociation constants less than 30%. Taking into account that, in general, measured dissociation constants often differ by orders of magnitude, the described assay is a useful method for determining these constants with sufficient accuracy and without the need of expensive equipment. This is particularly important when studying complex molecular interactions in cell biology and when correlating ligand–receptor binding properties with structural data of the involved proteins.

Although the binding to the plastic surface might induce a conformational change in the immobilized protein and thereby alter its binding affinity, it is notable that nearly identical dissociation constants within the experimental error were obtained with immobilized receptor (EARLI) and with immobilized ligand (reciprocal EARLI). In addition, we believe that a solid phase assay like the EARLI better reflects the physiological conditions that are characterized by the binding of a soluble ligand, i.e. transferrin, to a cell surface-bound receptor, i.e. TfR.

Previously published dissociation constants for the binding of human transferrin to whole cells or cell extracts varied by a factor of 240 [10–13]. A relatively weak binding was described by Brown et al. [10] for the binding of transferrin to human placental syncytiotrophoblast plasma membrane preparations (K_d = 20–29 nM) and by Shindelman et al. [11] for the binding of ^{125}I-transferrin to microsomal preparations of breast tumor tissue ($K_d = 1.1$ nM). Those low affinities might be explained by the presence of endogenous, unlabeled transferrin and of other receptors that bind transferrin with a lower affinity, like the asialoglycoprotein receptor [17,18] and the human transferrin receptor type 2 [35].

Using a Triton extract of an acetone powder from human placenta, Tsunoo et al. [12] determined a K_d of 1.3 nM that was corrected for the presence of endogenous transferrin by a model calculation leading to a final value of $K_d = 0.42$ nM. Even closer to our dissociation constant of 0.224 nM (average value of EARLI and reciprocal EARLI) is the measurement of Chitambar et al. [13] who determined a dissociation constant of $K_d = 0.12$ nM from an apparently transferrin-free supernatant of HL-60 cells by immunoprecipitating TfR and quantifying the coprecipitated transferrin. Thus the exclusion of endogenous transferrin and the reduction of the influence of other receptors appear to be prerequisites for the exact determination of dissociation constants.

A striking result of our study is the notable effect of iodination on the binding properties. The rate constant for the binding of iodinated transferrin is reduced by a factor of 2 and the affinity by a factor of 5. Similarly, the affinity of iodinated TfR to unmodified transferrin is reduced by a factor of 3. In contrast to iodination, the isotopic labeling of transferrin with $^{59}Fe^{3+}$ does not alter its chemical nature. Indeed, our results show (Fig. 2) that

^{59}Fe-transferrin binds with the same rate constant to the TfR as unlabeled transferrin.

The effect of iodination upon binding can be explained by the presence of not less than five tyrosine residues within the protein regions believed to form the ligand binding site of the human TfR [4]. The bulky iodine substituent increases the protein surface and its hydrophobicity. Thus, both the steric conditions and the microenvironment of the binding domain may contribute to the decreased association constant. Previously published studies with iodine-labeled protein ligands have shown that both the position of the label within the molecule [36] and the iodination method [37,38] influence receptor binding. However, regarding the magnitude of error introduced into the equilibrium constant by iodination, it appears feasible to avoid covalent labeling altogether and to use methods that do not rely on covalent labeling.

Beyond iodination, covalent labeling of biomolecules with fluorophores has become a very common tool in cell biology. Since fluorophores, such as fluorescein, are much more bulky than iodine, steric interference with molecular interactions must also be anticipated with this technique. The same precaution has to be considered when using other typical labeling reagents like biotin.

Our study reveals that covalent labeling of tyrosine residues with ^{125}I significantly alters the binding of transferrin to its receptor. This finding is in line with the geometry of the proposed ligand binding area of the human TfR. We conclude that covalent modifications have a significant impact on the strength of molecular interactions. The described assay for the quantitation of receptor–ligand interactions offers a useful alternative to other non-radioactive methods that require large equipment such as plasmon resonance technology.

Acknowledgements

This work was supported by the Deutsche Forschungsgemeinschaft (Sonderforschungsbereich 312, Teilprojekt D4).

References

[1] A. Dautry-Varsat, A. Ciechanover, H.F. Lodish, Proc. Natl. Acad. Sci. USA 80 (1983) 2258–2262.
[2] C.R. Hopkins, A. Gibson, M. Shipman, D.K. Strickland, I.S. Trowbridge, J. Cell Biol. 125 (1994) 1265–1274.
[3] S.Q. Jing, I.S. Trowbridge, EMBO J. 6 (1987) 327–331.
[4] C.M. Lawrence, S. Ray, M. Babyonyshev, R. Galluser, D.W. Borhani, S.C. Harrison, Science 286 (1999) 779–782.
[5] H. Fuchs, U. Lücken, R. Tauber, A. Engel, R. Geßner, Structure 6 (1998) 1235–1243.
[6] G. Orberger, R. Geyer, S. Stirm, R. Tauber, Eur. J. Biochem. 205 (1992) 257–267.
[7] G.R. Hayes, A.M. Williams, J.J. Lucas, C.A. Enns, Biochemistry 36 (1997) 5276–5284.
[8] S.I. Do, R.D. Cummings, Glycobiology 2 (1992) 345–353.
[9] G.R. Hayes, C.A. Enns, J.J. Lucas, Glycobiology 2 (1992) 355–359.
[10] P.J. Brown, C.M. Molloy, P.M. Johnson, Placenta 3 (1982) 21–28.
[11] J.E. Shindelman, A.E. Ortmeyer, H.H. Sussman, Int. J. Cancer 27 (1981) 329–334.
[12] H. Tsunoo, H.H. Sussman, J. Biol. Chem. 258 (1983) 4118–4122.
[13] C.R. Chitambar, Z. Zivkovic, Blood 74 (1989) 602–608.
[14] A. Ciechanover, A.L. Schwartz, A. Dautry-Varsat, H.F. Lodish, J. Biol. Chem. 258 (1983) 9681–9689.
[15] N. Gironès, R.J. Davis, Biochem. J. 264 (1989) 35–46.
[16] A. van der Ende, A. du Maine, A.L. Schwartz, G.J. Strous, Biochem. J. 270 (1990) 451–457.
[17] C.J. Dekker, M.J. Kroos, C. Van der Heul, H.G. Van Eijk, Int. J. Biochem. 17 (1985) 701–706.
[18] S.P. Young, A. Bomford, R. Williams, J. Biol. Chem. 258 (1983) 4972–4976.
[19] M. Hugues, D. Duval, P. Kitabgi, M. Lazdunski, J.P. Vincent, J. Biol. Chem. 257 (1982) 2762–2769.
[20] R. Mattera, D. Turyn, H.N. Fernandez, J.M. Dellacha, Int. J. Pept. Protein Res. 19 (1982) 172–180.
[21] C. Hofmann, P. Luthy, R. Hutter, V. Pliska, Eur. J. Biochem. 173 (1988) 85–91.
[22] I. Virgolini, P. Angelberger, S.R. Li, F. Koller, E. Koller, J. Pidlich, G. Lupattelli, H. Sinzinger, J. Nucl. Med. 32 (1991) 2132–2138.
[23] H. Fuchs, G. Orberger, R. Tauber, R. Geßner, J. Immunol. Methods 188 (1995) 197–208.
[24] H. Fuchs, R. Geßner, R. Tauber, R. Ghosh, Biochemistry 34 (1995) 6196–6207.
[25] M. Karin, B. Mintz, J. Biol. Chem. 256 (1981) 3245–3252.
[26] A.P. Turkewitz, J.F. Amatruda, D. Borhani, S.C. Harrison, A.L. Schwartz, J. Biol. Chem. 263 (1988) 8318–8325.
[27] P.J. Fraker, J.C. Speck Jr, Biochem. Biophys. Res. Commun. 80 (1978) 849–857.
[28] H. Gallati, I. Pracht, J. Clin. Chem. Clin. Biochem. 23 (1985) 453–460.
[29] H. Fuchs, R. Geßner, Biochem. J. 359 (2001) 411–418.
[30] U.K. Laemmli, Nature 227 (1970) 680–685.
[31] E. Alvarez, N. Gironès, R.J. Davis, J. Biol. Chem. 265 (1990) 16644–16655.
[32] R.J. Davis, G.L. Johnson, D.J. Kelleher, J.K. Anderson, J.E. Mole, M.P. Czech, J. Biol. Chem. 261 (1986) 9034–9041.
[33] Y.J. Shih, R.D. Baynes, B.G. Hudson, C.H. Flowers, B.S. Skikne, J.D. Cook, J. Biol. Chem. 265 (1990) 19077–19081.
[34] G. Scatchard, Ann. NY Acad. Sci. 51 (1949) 660–672.
[35] H. Kawabata, R. Yang, T. Hirama, P.T. Vuong, S. Kawano, A.F. Gombart, H.P. Koeffler, J. Biol. Chem. 274 (1999) 20826–20832.
[36] J.L. Diaz, T.J. Wilkin, Clin. Chem. 34 (1988) 356–359.
[37] A.B. Mason, S.A. Brown, Biochem. J. 247 (1987) 417–425.
[38] C.B. Kienhuis, J.J. Heuvel, H.A. Ross, L.M. Swinkels, J.A. Foekens, T.J. Benraad, Clin. Chem. 37 (1991) 1749–1755.